ARTICLES

Carbon nanotubes assisting interchain charge transport in semiconducting polymer thin films towards much improved charge carrier mobility

Zhe Zheng[1,2], Zhenjie Ni[2], Xiaotao Zhang[1], Yonggang Zhen[2], Huanli Dong[2*], Jin Zhang[3*] and Wenping Hu[1,2*]

ABSTRACT Conjugated polymers attracted much attention in the past few decades due to their wide applications in various optoelectronic devices and circuits. The charge transport process in conjugated polymers mainly occurs in the intrachain and interchain parts, where the interchain charge transport is generally slower than intrachain transport and may slow down the whole charge transport properties. Aiming at this issue, herein we employ semiconducting single-walled carbon nanotubes (s-SWNTs) as efficient charge-transporting jointing channels between conjugated polymer chains for improving the charge transport performance. Taking the typical conjugated polymer, ploy-*N*-alkyl-diketopyrrolo-pyrrole-dithienylthieno[3,2-*b*]thiophene (PDPP-TT) as an example, polymer thin film transistors (PTFTs) based on the optimized blended films of PDPP-TT/s-SWNTs exhibit an obviously increasing device performance compared with the devices based on pure PDPP-TT films, with the hole and electron mobility increased from 2.32 to 12.32 $cm^2\ V^{-1}\ s^{-1}$ and from 2.02 to 5.77 $cm^2\ V^{-1}\ s^{-1}$, respectively. This result suggests the importance of forming continuous conducting channels in conjugated polymer thin films, which can also be extended to other polymeric electronic and optoelectronic devices to promote their potential applications in large-area, low-cost and high performance polymeric electronic devices and circuits.

Keywords: conjugated polymer, s-SWNTs, connected conducting channel, carrier mobility

INTRODUCTION

Organic conjugated polymers play an important role in the electronic devices. The properties such as low cost, high production and easy processing make them hopeful in the applications of various fields [1–8]. Their physical properties, for instance bandgaps, energy levels and Fermi energy can be easily tuned by changing the conjugated polymer structures. Currently, most of polymer electronic and optoelectronic devices are based on the spin-coated polymer thin films. In these cases, the polymer chains are generally in highly disordered conformation, which usually leads to severe decrease in charge transport property of the devices because charged carriers may be slowed down as they hop between the chains and across the disordered chain fragments [9,10]. Conjugated polymers are intrinsically one-dimensional chains, and it is widely accepted that if there is efficient electron delocalization along the conjugated polymer backbones determined by the regularity and planar-conformation of polymer backbones [11–16], the intrachain charge transport should be much faster than interchain charge transport (the hopping transport between the chains) [11,12,16]. So over the past years, extensive efforts were devoted to this field to optimize the solid state structures of conjugated polymers with the aim of getting uniaxially aligned polymer chains by constructing aligned conjugated polymer films [11,12,16,17–20], which have been proved to indeed improve the charge transport and

---

[1] Tianjin Key Laboratory of Molecular Optoelectronic Science, Department of Chemistry, School of Science, Tianjin University and Collaborative Innovation Center of Chemical Science and Engineering (Tianjin), Tianjin 300072, China

[2] Beijing National Laboratory for Molecular Sciences, Key Laboratory of Organic Solids, Institute of Chemistry, Chinese Academy of Sciences, Beijing 100190, China

[3] Center for Nanochemistry, Beijing Science and Engineering Center for Nanocarbons, Beijing National Laboratory for Molecular Sciences (BNLMS), College of Chemistry and Molecular Engineering, Peking University, Beijing 100871, China

* Corresponding authors (emails: huwp@tju.edu.cn (Hu W); dhl522@iccas.ac.cn (Dong H); jinzhang@pku.edu.cn (Zhang J))

optoelectronic property along the polymer chain orientation compared with that of the corresponding spin-coated thin films. One of the examples is that the polymer field-effect transistors (PFETs) based on aligned poly[4-(4,4-dihexadecyl-4H-cyclopenta[1,2-b:5,4-*b'*] di-thiophen-2-yl) (PCDTPT) thin films exhibit a high charged carrier mobility up to 36.3 cm^2 V^{-1} s^{-1}. The mobility could even be much higher (58.6 cm^2 V^{-1} s^{-1}) due to the highly ordered polymer chain and the proper molecular mass [21,22]. In addition, recently the development of conjugated polymer crystals that have long-range molecular orders and crystal boundaries offered the potential to further increase the charge transport performance as well as carry out fundamental investigations in conjugated polymers [11,23–28]. More recently, Yao *et al.* [12] have generated high quality conjugated polyacetylene micro/nano- single crystals using a surface supported topochemical polymerization method, which not only exhibit efficient charge transport along the conjugated polymer backbone direction (carrier mobility up to 42.7 cm^2 V^{-1} s^{-1}), but also for the first time realize the fundamental anisotropic charge transport property based an individual conjugated polymer crystal. Although significant advance has been achieved for the improvement of charge transport performance and fundamental physical studies of the uniaxially oriented conjugated polymer films and crystals, the preparation of large-area high quality oriented polymer films and single crystals through a simple and robust approach remains challenging, which to some extent limits their potential applications in organic electronics. Therefore, it is worth developing a simple and robust approach for high performance polymer electronic devices.

As mentioned above, the hopping process between chains may slow down the whole charge transport performance, so efficient charge-transporting jointing channels in conjugated polymer films are crucial for the enhancement of charge transport property. Liu *et al.* [29] demonstrated that the polymer/graphene composites showed increased charge transport property due to the reduced π-π stacking distance between graphene and the polymer. Herein we propose a new concept to build quick interchain transport channels for efficient interchain charge-transporting between the conjugated polymer chains by incorporating semiconducting single-walled carbon nanotubes (s-SWNTs). The selection of s-SWNTs is based on the following considerations: i) the formation of intact π-π interactions between carbon nanotubes and conjugated polymer chains by tightly wrapping [30,31] due to their similar large π-conjugation structures and ii)

the capability of providing extra carriers and fast carrier transport of s-SWNTs [32,33] to improve the resulting electrical performance. In the previous research [34], s-SWNTs interlayers were used by Lee *et al.* to reduce the contact resistance between electrodes and organic semiconducting layers. In this work, we employed s-SWNTs as a linker mixed directly in the network of organic polymer to enhance the interchain charge transport. Taking the typical conjugated polymer, poly-*N*-alkyl-diketopyrrolo-pyrrole-dithienylthieno[3,2-*b*]thiophene (PDPP-TT) as an example, the bottom-contact top-gate (BCTG) polymer thin film transistors (PTFTs) constructed by the optimized blended films of PDPP-TT and s-SWNTs exhibit an obvious increase (3–5 times) in both hole and electron carrier mobility compared with the devices based on pure PDPP-TT films due to the formation of continuous conducting channels in the blended films. This result clearly confirms the importance of continuous conducting channels in conjugated polymer thin films for the high electrical performance. This concept based on PDPP-TT can also be extended to other polymeric electronic and optoelectronic π-conjugated polymer systems for high performance devices at large scale with low cost.

EXPERIMENTAL SECTION

Preparation of PTFTs
The polyethylene terephthalate (PET) substrates were cut into 1.5 cm×1.5 cm square followed by being cleaned in sonication. The washing process was in the sequence of deionized water for twice and isopropanol for once and each step cost 10 min. After cleaning step, the mask was labelled on PET and gold (Au) electrodes were thermally evaporated on the substrates with 15 nm thickness as drain and source electrodes. Next, the thin-film was spin-coated on the substrates after being blown under nitrogen gas for several seconds. The spin-coating was carried out under 1,800 revolutions per minute (RPM) for 1 min followed by annealing in ambient atmosphere for 10 min at 200°C. Then, a dielectric layer, polymethyl methacrylate (PMMA), was spin-coated on the substrates under 3,200 RPM for 1 min followed by annealing in ambient atmosphere for 30 min at 90°C. Finally, the top gate electrodes aluminium (Al) was thermally evaporated on the PMMA in the thickness of 100 nm with the assistance of matched mask. In addition, PDPP-TT was dissolved in 1,2-dichlorobenzene (1,2-DCB) and the concentration was 4 mg mL^{-1} while PMMA was dissolved in *n*-butyl acetate and the concentration was 60 mg mL^{-1}.

Preparation of PDPP-TT and s-SWNTs

The synthesis of PDPP-TT was reported in previous work [35]. The s-SWNTs was dissolved with poly [9-(1-octylonoyl)-9H-carbazole-2,7-diyl] (PCz) in toluene in the ratio of 1:2:4. Then ultrasonication was carried out at a power of 300 W for 1 h. After that, the supernate and the impurity were separated by ultracentrifugation at 20k RPM for 2 h. Then the supernate was filtered by vacuum filtration and washed with toluene for thrice, and thus the residual PCz was removed, and the s-SWNTs were located on the Teflon filter membrane with 0.1 μm pore.

Method to mix PDPP-TT and s-SWNTs

The membrane containing the s-SWNTs was put into 10 mL toluene, and then 100 μL PDPP-TT dissolved in 1,2-DCB was dropped into the solution. The s-SWNTs were moved away from the membrane by ultrasonication and re-dispersed into a solution to form the PDPP-TT wrapped on the s-SWNTs simultaneously. Next, the bundle and impurity were disposed by ultracentrifugation at 40k RPM. The supernatant was dropped into PDPP-TT solution and the mixture stood still for 24 h to make them mixed well. The final concentration of PDPP-TT in the mixture was 4 mg mL^{-1} and that of the s-SWNTs was about 40 μg mL^{-1}.

Characterization of samples

The atomic force microscopy (AFM) images were obtained in a square of 1 μm×1 μm under peak force tapping mode with Bruker Dimension Icon. The Raman spectra were obtained under a 532 nm laser on the glass substrate for eliminating the influence of PET by using Horiba LabRAM HR800. The ultraviolet-visible-near infrared (UV-vis-NIR) absorption spectra were measured on the double-sided polishing quartz from 300 to 2,000 nm by Shimadzu UV3600 Plus UV-VIS-NIR SPECTRO-PHOTOMETER. All of the materials were handled with the same method mentioned above.

Measurement of electrical property of PTFTs

The transfer and output characteristic curves were measured with Micromanipulator Keithley MM6200-4200/SCS under the ambient atmosphere at room temperature. The p-type transfer characteristic curve was tested under −40 V bias voltage and the gate voltage swept from 10 to −60 V while n-type was under 40 V bias and the gate voltage swept from −10 to 60 V. In the p-type output characteristic curve the drain-source voltage was from 10 to −60 V and gate voltage changed from 0 to −40 V by a step of −10 V. In the n-type output characteristic curves, the drain-source voltage was from −10 to 60 V and gate voltages changed from 0 to 80 V by a step of 20 V.

Calculation of mobility of hole (μ_h) and electron (μ_e)

The mobility was calculated with Equation (1), the classic equation, in saturation region. In the equation, L and W are the length and width of channel, respectively. C_i stands for capacitance per area of dielectric and is 3.3 nF m^{-1} in this condition. $\partial \sqrt{I_{SD}} / \partial V_G$ can be fitted from the slope of the transfer characteristic curve $(-I_{SD})^{1/2}$ $-V_G$.

$$\mu = \frac{2L}{WC_i}\left(\frac{\partial \sqrt{I_{SD}}}{\partial V_G}\right). \tag{1}$$

RESULTS AND DISCUSSION

Here, PDPP-TT as a kind of representative semiconducting polymers with extended π-conjugation backbone and high electrical properties [35,36] is selected to investigate the effect of incorporating s-SWNTs charge-transporting jointing channels in polymer films on the resulting charge transport performance. The PDPP-TT polymer has a mass average molar mass of 1.14×10^5 with a polydispersity index (PDI) of 1.60 estimated by gel permeation chromatography (GPC) with polystyrene as the calibration standard and 1,2-DCB as the eluent at 140°C. The s-SWNTs were obtained from selective dispersion with the assistance of PCz. Ultrasonication and ultracentrifugation were carried out to obtain the highly pure (99.9%) s-SWNTs [30]. As shown in Fig. 1a, the BCTG PTFTs contain PET as the substrate, Au as the drain and source electrodes, PMMA as the dielectric layer and Al as the top gate electrode. By comparison, we spin-coated the active layer of PDPP-TT films with and without s-SWNTs respectively to fabricate the devices.

As shown in Fig. 1b, in the pure PDPP-TT films, the polymer chains intertwine with each other and the interchain transport may occur at the random contact (as shown by the red circles) which is unfavorable for the efficient charge transport in the resulting films. In addition to the appropriate amount of s-SWNTs into the polymer films, the π-π conjugated system and cylinder conformation of s-SWNTs lead to the strong interaction between polymers and the s-SWNTs as conducting "bridge" linking in the polymer networks by tightly wrapping in their joints. Moreover, s-SWNTs also show a quick transport and provide extra carriers modulated by the gate voltage, which further promotes the electrical property of the devices. Therefore, the
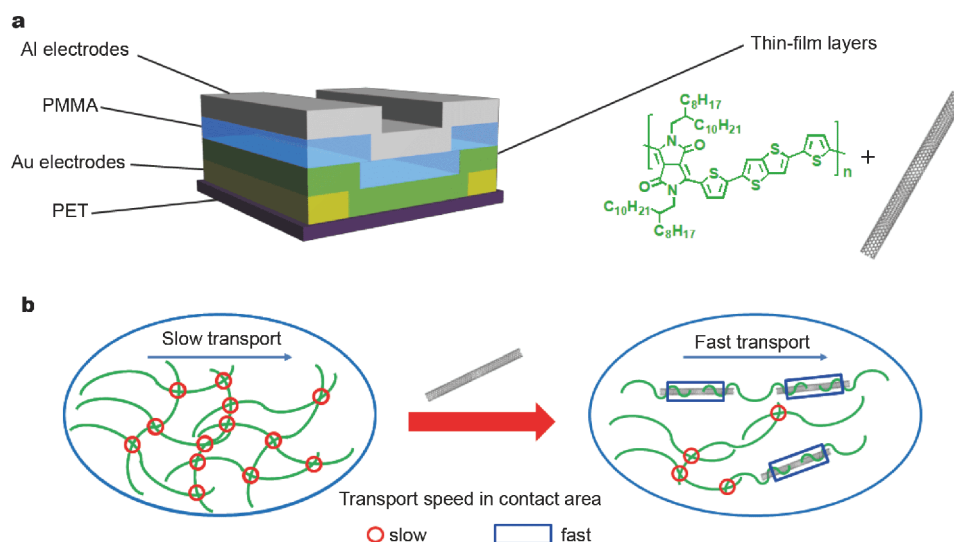
Figure 1 (a) The illustration of BCTG PTFT. (b) With the introduction of s-SWNTs, the movement path of charge carriers changed from a loose contact between the polymers to tough contact of polymer and s-SWNTs. Besides, a brief model shows a slow transport (red circle) in PDPP-TT interchain transport and fast transport (blue rectangle) in the PDPP-TT/s-SWNTs interchain transport.

charge carrier transport in PDPP-TT/s-SWNTs devices is expected to be fast when the continuous channels are constructed by s-SWNTs as shown by the blue rectangle.

In our preliminary experiments, if the s-SWNTs were simply mixed with polymers and then spin-coated, the resulting devices based on blended PDPP-TT/s-SWNTs films exhibited decreased mobility, μ_h and μ_e, of 0.40 and 0.31 cm^2 V^{-1} s^{-1}, respectively (Fig. S1), compared with those based on pure PDPP-TT. It is inferred that the simple mixing process does not work effectively as the polymer and s-SWNTs cannot be combined with each other but isolated in the film. While the rough mixing process did not improve the interchain contact between the polymers and charge carriers transport because the original stacking regularity of polymer was ruined. To form a tight contact between the PDPP-TT polymer chains and s-SWNTs, we utilized ultrasonication to increase the collision probability of polymer and s-SWNTs in the solution as well as to make polymers cling to or wrap on s-SWNTs by high power [30,31], as shown in Fig. 2a. The key point in this ultrasonication process is that the polymer and s-SWNTs can form a mixture with tight contact instead of two isolated materials.

The blended films consist of large amounts of polymer with incorporation of a small amount of s-SWNTs (as small as 1 wt.%), which is just used for the formation of connecting joints. The morphology of the film with s-SWNTs (~1 wt.%) shows negligible change as measured by AFM, as shown in Fig. 2b, c. The existence of s-

SWNTs was proved by Raman and UV-vis-NIR absorption spectra. As shown in Fig. 2d, the Raman spectrum of the blended films shows a peak at 1,590 cm^{-1} in the red line, which is a typical characteristic G-peak of carbon nanotubes. The inset is the magnified region which shows a clear difference at 1,590 cm^{-1} between the two films. In Fig. 2e, UV-vis-NIR absorption spectra of PDPP-TT/s-SWNTs demonstrate the typical peaks of both PDPP-TT and s-SWNTs. The absorption peaks between 800 and 900 nm are attributed to PDPP-TT polymer, while the peaks between 1,000 and 1,200 nm originate from the S$_{22}$ absorption of arc discharge s-SWNTs, and those between 1,600 and 2,000 nm are from S$_{11}$ absorption. The inset shows the absorption of s-SWNTs in the suitable scale. Besides, to prove the combination of polymer and s-SWNTs, we measured the UV-vis-NIR absorption spectra of s-SWNTs before and after ultrasonication. The s-SWNTs were deposited on the double-sided polishing quartz by dipping the substrate in the solution and then residual polymers on the substrate were eliminated by washing in tetrahydrofuran (THF). Fig. S2 shows that the UV-vis-NIR spectrum with ultrasonication process contains the absorption peak belonging to PDPP-TT between 800 and 900 nm which does not exist in the spectrum without the incorporation. That means a few dose of PDPP-TT was toughly twined on s-SWNTs by ultrasonication and not eliminated by the washing process. The results show ultrasonication can combine PDPP-TT and s-SWNTs
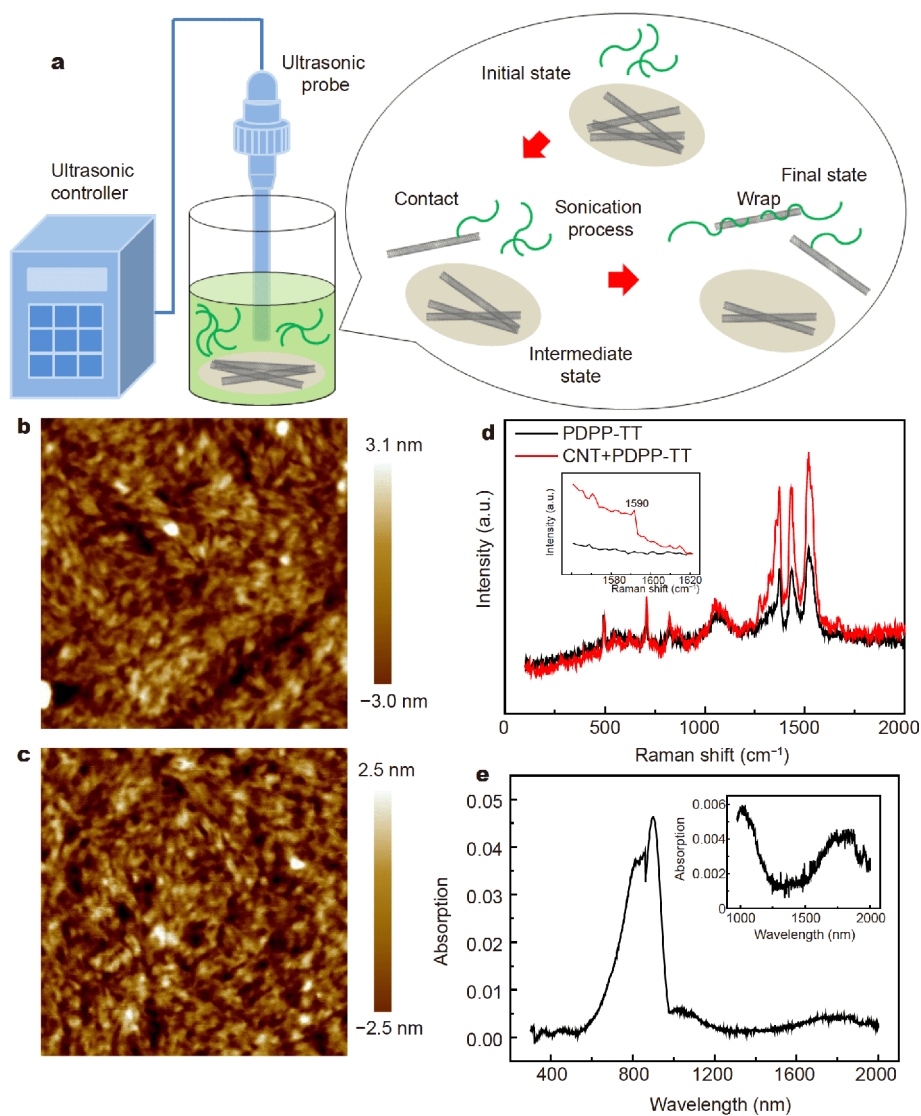
Figure 2 (a) The process for combination of polymer and s-SWNTs under ultrasonication with the probe dipped into solution. In the initial state, the polymer existed in the solution and the s-SWNTs laid on the filter membrane. With the sonication going on, the s-SWNTs started to leave the membrane and collided with polymers which then wrapped tightly on the s-SWNTs finally. AFM images of (b) polymer and (c) polymer combined with s-SWNTs; (d) Raman spectrum of two kinds of materials, and the inset is 1,590 cm^{-1} peak attributed to G-peak of s-SWNTs; (e) UV-vis-NIR spectrum of polymer combined with s-SWNTs on the double-sided polishing quartz, and the inset is the S$_{11}$ (1,600–2,000 nm) and S$_{22}$ (1,000–1,200 nm) absorption of s-SWNTs.

through π-π stacking by the great power. It is vital to improve the property of PTFTs.

To investigate the electrical property of the optimized blended films, both BCTG PTFTs with PDPP-TT/s-SWNTs and pure PDPP-TT were fabricated and measured under the same conditions. The transfer and output characteristic curves of p-type and n-type electrical performance of the PDPP-TT/s-SWNTs PTFTs are shown in Fig. 3a–d, respectively. And the corresponding characteristic curves of the PDPP-TT PTFTs are shown in Fig. 3e–h. Through the transfer characteristic curve, the calculated highest μ_h and μ_e are up to 12.32 and 5.77 cm^2 V^{-1} s^{-1} respectively for the blended PDPP-TT/s-SWNTs film-based devices while the μ_h and μ_e of PDPP-TT are 2.32 and 2.02 cm^2 V^{-1} s^{-1}, respectively. Compared with that of pure PDPP-TT-based PTFTs in the same condition, the μ_h and μ_e of PDPP-TT PTFTs increased approximately 5 and 3 times respectively with the introduction of s-SWNTs, and the enhancement in the charge transport is also further evidenced by their
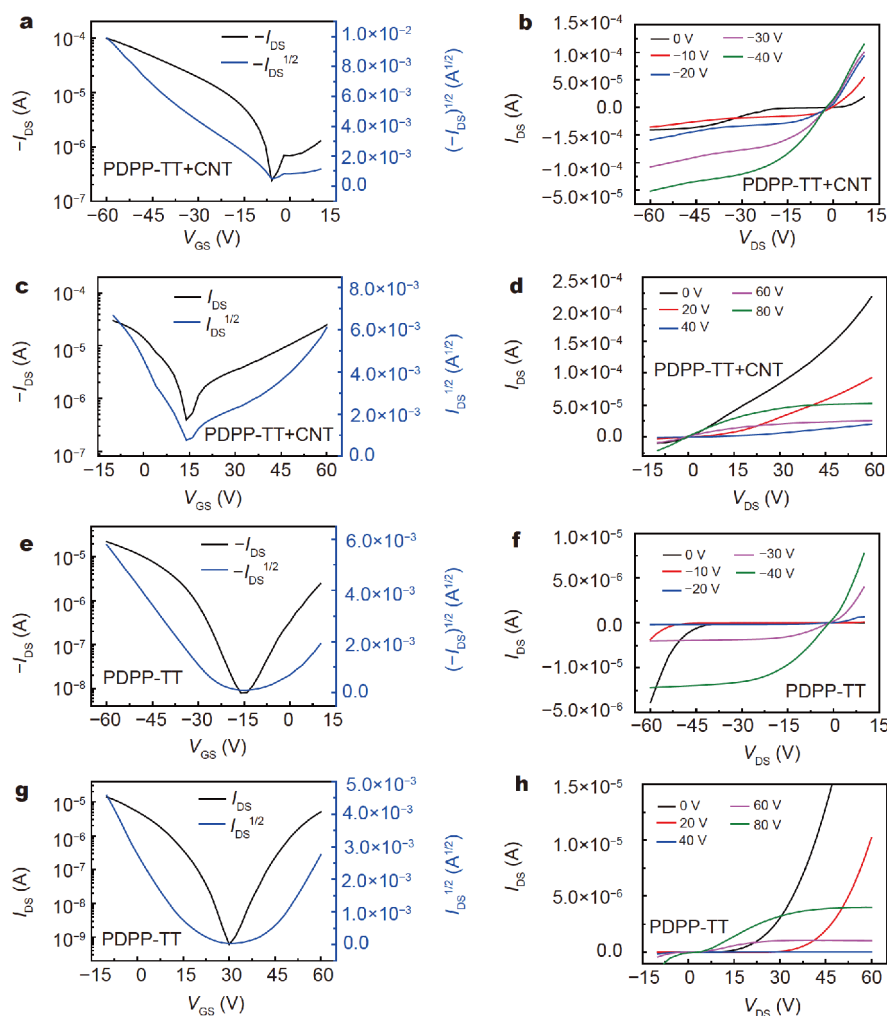
Figure 3 (a, b) The p-type transfer and output characteristic curves of the devices based on PDPP-TT/s-SWNTs; (c, d) the n-type transfer and output characteristic curves of the devices based on PDPP-TT/s-SWNTs. (e–h) The corresponding transfer and output characteristic curves of the devices based on PDPP-TT.

conductance through the I–V curves (Fig. S3). We optimized the resulting device performances with different concentrations of s-SWNTs (1 wt.%, 0.5 wt.%, 0.33 wt.%, 0.25 wt.% and 0.2 wt.%). The results demonstrate that under the concentration of 1 wt.% s-SWNTs, the devices exhibit the best performances, which may be due to the effective connection of s-SWNTs and polymer networks, thus resulting in the efficient interchain charge transport in the devices (Fig. S4). Moreover, it should be stated that considering the short length (1–2 μm) and small amount (1 wt.%) of s-SWNTs in polymer films, it is impossible to form continuous s-SWNTs network connecting between source and drain electrode (a relatively large channel length of 20 μm). That is to say, the enhancement of the charge transport in

the s-SWNTs/polymer films is due to the efficient interchain charge transport on account of the bridging effect of s-SWNTs between polymer chains. To eliminate the interference of leakage current, the gate currents of both were also tested. The results show the leakage gate current is usually in the range of 10^{-11}–10^{-10} A or even lower values of 10^{-12}–10^{-11} A, which means characteristic curves of the devices based on PDPP-TT/s-SWNTs and PDPP-TT are credible. Besides, the influence of metallic (m-) SWNTs can be also negligible because the residual of them is tiny because the Raman and UV-vis-NIR absorption spectra (Figs S5, S6) show the absence of m-SWNTs. Besides, the electrical properties, transfer and output characteristic curves (Fig. S7) of the devices based on SWNTs also show the high purity of s-SWNTs. Thus,
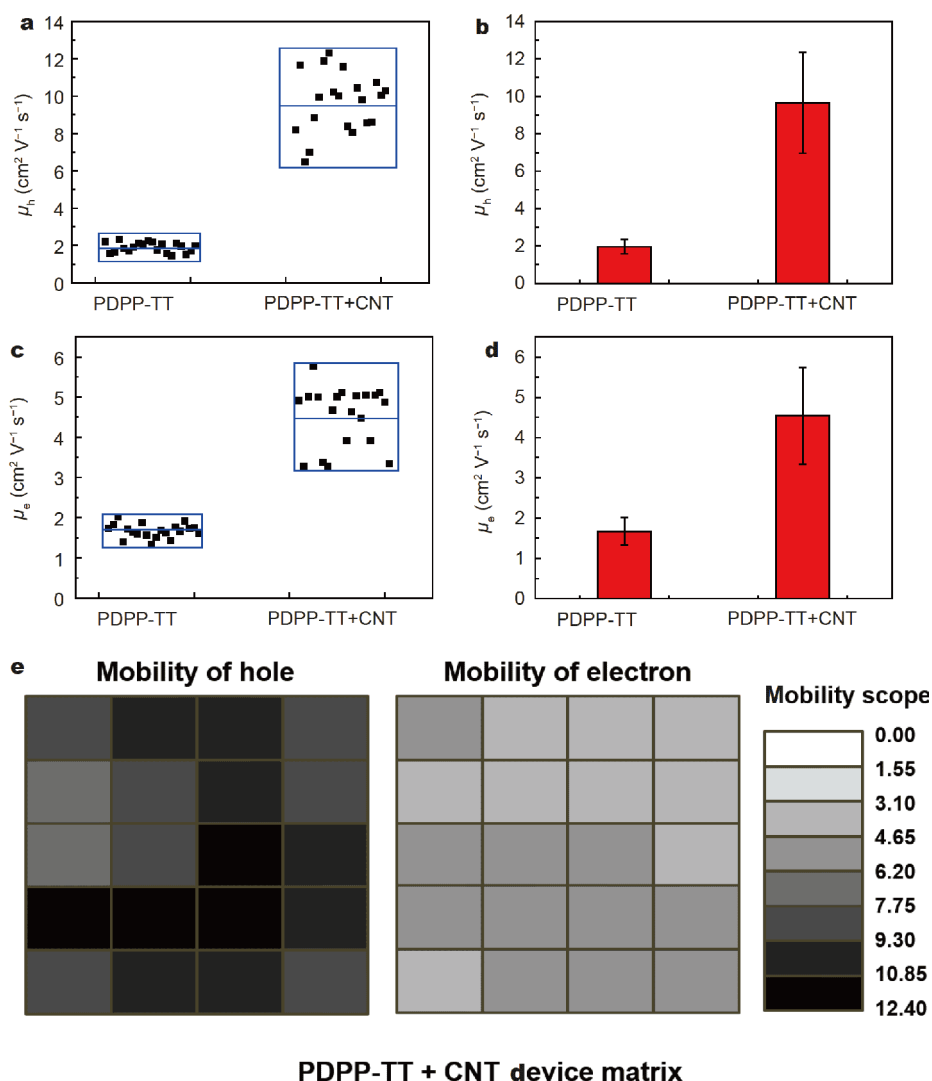
Figure 4 The statistical data of mobility of two kinds of materials, (a) scatter diagram and (b) bar graph of μ_h; (c) scatter diagram and (d) bar graph of μ_e. (e) The 2D distribution diagram of μ_h and μ_e of devices based on PDPP-TT/s-SWNTs, which shows the good uniformity of mobility.

the electrical properties of PDPP-TT/s-SWNTs devices do not come from experiment error or impurity. The result further demonstrates that optimizing the mixing condition is of great importance for the formation of blended films and the resulting electrical performance.

PTFTs fabricated in different conditions were measured and the statistical data regarding the μ_h and μ_e for pure polymer films and PDPP-TT/s-SWNTs blended films are shown in Fig. 4. In the typical data derived from two-group devices fabricated simultaneously that one was based on pure PDPP-TT films and the other used PDPP-TT/s-SWNTs blended films, the results demonstrate an obvious increase of the charge transport for the blended films devices. Fig. 4a, b show the scatter diagram and bar

graph of μ_h, respectively. The PTFTs based on PDPP-TT exhibit μ_h with less deviation while those based on PDPP-TT/s-SWNTs have more discrete μ_h. The average values of μ_h of PDPP-TT and PDPP-TT/s-SWNTs are 1.97 and 9.65 cm^2 V^{-1} s^{-1}, respectively. The same phenomenon also appears in μ_e of the two kinds of devices, as shown in Fig. 4c, d. The calculated average μ_e values of PDPP-TT and PDPP-TT/s-SWNTs are 1.67 and 4.54 cm^2 V^{-1} s^{-1}, respectively. The μ_h ranges from 6.47 to 12.32 cm^2 V^{-1} s^{-1} and μ_e ranges from 3.27 to 5.77 cm^2 V^{-1} s^{-1} in PDPP-TT/s-SWNTs devices. By comparison, the mobility of PDPP-TT devices changes less. The μ_h ranges from 1.58 to 2.32 cm^2 V^{-1} s^{-1} and μ_e ranges from 1.33 to 2.02 cm^2 V^{-1} s^{-1}. The detailed field-effect parameters for

the different devices are summarized in Table S1 and S2. Except for PDPP-TT polymer, this research concept can be also extended to other conjugated polymer systems, such as an asymmetric thiophene/pyridine flanked DPP-based polymer (PPyTDPP-BT), as shown in Fig. S8 [37] and the corresponding experimental data are shown in Figs S9–S11. The results also demonstrate a similar increase, suggesting it is a universal method for constructing high performance polymeric electronic devices.

The good uniformity of the mobility of PTFTs based on such blended PDPP-TT/s-SWNTs films over a 7 mm width × 6 mm height area is figured out from the two dimension (2D) mobility distribution diagram (Fig. 4e). The corresponding optical image of 4×5 device arrays is shown in Fig. S12. Obviously, all the devices in the array can successfully operate and a majority of the devices show similar performance, revealing a small device-to-device variation in μ_h and μ_e with small standard deviations of ±2.93 and 1.25 cm^2 V^{-1} s^{-1}, respectively. The good device uniformity of blended PDPP-TT/s-SWNTs films-based PTFT arrays suggests their great potential applications in the solution-processing of large-area, low-cost flexible polymeric electronic and optoelectronic devices and circuits with high efficiency, such as ink-jet printing, blade shearing and other solution-processing methods.

CONCLUSIONS

In this work, we demonstrate that a small amount of s-SWNTs in the conjugated polymer films can significantly increase the charge transport performance due to the constructed efficient charge-transporting jointing channels. As an example, the PTFTs based on PDPP-TT/s-SWNTs films prepared through ultrasonication process exhibit a hole and electron mobility up to 12.32 and 5.77 cm^2 V^{-1} s^{-1}, respectively, which are obviously 3–5 times higher than pure PDPP-TT film based devices. Large-area PTFTs fabricated based on the blended PDPP-TT/s-SWNTs films also demonstrate good device uniformity with small device-to-device variation. This concept has also been extended to other conjugated polymer systems, such as PPyTDPP-BT, which suggests the great potential of this approach in large-area, low-cost solution-processing high-performance polymeric electronic and optoelectronic devices/circuits.

1 Facchetti A. π-Conjugated polymers for organic electronics and photovoltaic cell applications. Chem Mater, 2011, 23: 733–758

2 Hu WP. Organic Optoelectronics. Weinheim: Wiley-VCH, 2012

3 Feng LL, Gu PC, Yao YF, et al. High-mobility polymeric semiconductors. Chin Sci Bull (Chin Ver), 2015, 60: 2169–2187

4 Yang J, Zhao Z, Wang S, et al. Insight into high-performance conjugated polymers for organic field-effect transistors. Chem, 2018, 4: 2748–2785

5 Qian Y, Zhang X, Qi D, et al. Thin-film organic semiconductor devices: from flexibility to ultraflexibility. Sci China Mater, 2016, 59: 589–608

6 Liu D, Chu Y, Wu X, et al. Side-chain effect of organic semiconductors in OFET-based chemical sensors. Sci China Mater, 2017, 60: 977–984

7 Xie J, Zhao CE, Lin ZQ, et al. Nanostructured conjugated polymers for energy-related applications beyond solar cells. Chem Asian J, 2016, 11: 1489–1511

8 Xie J, Wang Z, Gu P, et al. A novel quinone-based polymer electrode for high performance lithium-ion batteries. Sci China Mater, 2016, 59: 6–11

9 Jiang L, Sun Y, Peng H, et al. Enhanced electrical conductivity of individual conducting polymer nanobelts. Small, 2011, 7: 1949–1953

10 Sirringhaus H, Bird M, Zhao N. Charge transport physics of conjugated polymer field-effect transistors. Adv Mater, 2010, 22: 3893–3898

11 Dong H, Hu W. Multilevel investigation of charge transport in conjugated polymers. Acc Chem Res, 2016, 49: 2435–2443

12 Yao Y, Dong H, Liu F, et al. Approaching intra- and interchain charge transport of conjugated polymers facilely by topochemical polymerized single crystals. Adv Mater, 2017, 29: 1701251

13 Yao Y, Dong H, Hu W. Charge transport in organic and polymeric semiconductors for flexible and stretchable devices. Adv Mater, 2016, 28: 4513–4523

14 Collins BA, Cochran JE, Yan H, et al. Polarized X-ray scattering reveals non-crystalline orientational ordering in organic films. Nat Mater, 2012, 11: 536–543

15 Clark J, Silva C, Friend RH, et al. Role of intermolecular coupling in the photophysics of disordered organic semiconductors: aggregate emission in regioregular polythiophene. Phys Rev Lett, 2007, 98: 206406

16 Sirringhaus H. Device physics of solution-processed organic field-effect transistors. Adv Mater, 2005, 17: 2411–2425

17 Shao W, Dong H, Jiang L, et al. Morphology control for high performance organic thin film transistors. Chem Sci, 2011, 2: 590–600

18 Liu S, Wang WM, Briseno AL, et al. Controlled deposition of crystalline organic semiconductors for field-effect-transistor applications. Adv Mater, 2009, 21: 1217–1232

19 Dong H, Li H, Wang E, et al. Ordering rigid rod conjugated polymer molecules for high performance photoswitchers. Langmuir, 2008, 24: 13241–13244

20 Yao Y, Dong H, Hu W. Ordering of conjugated polymer molecules: recent advances and perspectives. Polym Chem, 2013, 4: 5197–5205

21 Luo C, Kyaw AKK, Perez LA, et al. General strategy for self-assembly of highly oriented nanocrystalline semiconducting polymers with high mobility. Nano Lett, 2014, 14: 2764–2771

22 Takacs CJ, Treat ND, Krämer S, et al. Remarkable order of a high-performance polymer. Nano Lett, 2013, 13: 2522–2527

23 Dong H, Jiang S, Jiang L, et al. Nanowire crystals of a rigid rod

conjugated polymer. J Am Chem Soc, 2009, 131: 17315–17320

24 Lim JA, Liu F, Ferdous S, et al. Polymer semiconductor crystals. Mater Today, 2010, 13: 14–24

25 Dong H, Yan Q, Hu W. Multilevel investigation of charge transport in conjugated polymers-new opportunities in polymer electronics. Acta Polym Sin, 2017, 8: 1246–1260

26 Gu P, Hu M, Ding S, et al. High performance organic transistors and phototransistors based on diketopyrrolopyrrole-quaterthiophene copolymer thin films fabricated via low-concentration solution processing. Chin Chem Lett, 2018, 29: 1675–1680

27 Gu P, Yao Y, Dong H, et al. Preparation, characterization and field-effect transistor applications of conjugated polymer micro/nano-crystal. Acta Polym Sin, 2014, 8: 1029–1040

28 Feng L, Dong H, Li Q, et al. Tuning crystal polymorphs of a π-extended tetrathiafulvalene-based cruciform molecule towards high-performance organic field-effect transistors. Sci China Mater, 2017, 60: 75–82

29 Liu Y, Hao W, Yao H, et al. Solution adsorption formation of a π-conjugated polymer/graphene composite for high-performance field-effect transistors. Adv Mater, 2018, 30: 1705377

30 Gu J, Han J, Liu D, et al. Solution-processable high-purity semiconducting SWCNTs for large-area fabrication of high-performance thin-film transistors. Small, 2016, 12: 4993–4999

31 Liu D, Li P, Yu X, et al. A mixed-extractor strategy for efficient sorting of semiconducting single-walled carbon nanotubes. Adv Mater, 2017, 29: 1603565

32 Javey A, Guo J, Wang Q, et al. Ballistic carbon nanotube field-effect transistors. Nature, 2003, 424: 654–657

33 Dürkop T, Getty SA, Cobas E, et al. Extraordinary mobility in semiconducting carbon nanotubes. Nano Lett, 2004, 4: 35–39

34 Lee SH, Khim D, Xu Y, et al. Simultaneous improvement of hole and electron injection in organic field-effect transistors by conjugated polymer-wrapped carbon nanotube interlayers. Sci Rep, 2015, 5: 10407

35 Li J, Zhao Y, Tan HS, et al. A stable solution-processed polymer semiconductor with record high-mobility for printed transistors. Sci Rep, 2012, 2: 754

36 Yang J, Chen J, Sun Y, et al. Design and synthesis of novel conjugated polymers for applications in organic field-effect transistors. Acta Polym Sin, 2017, 7: 1082–1096

37 Qiu G, Jiang Z, Ni Z, et al. Asymmetric thiophene/pyridine flanked diketopyrrolopyrrole polymers for high performance polymer ambipolar field-effect transistors and solar cells. J Mater Chem C, 2017, 5: 566–572

Author contributions   Hu W, Zhang J and Dong H supervised the project and designed the experiment. Zheng Z performed the experiments with support from Dong H and Hu W. Ni Z provided the polymers and gave instruction in the fabrication of polymer device. Zhang J's group provided the s-SWNTs. Zhang X and Zhen Y gave valuable suggestion during the characterizations. Zheng Z and Dong H wrote the manuscript and all authors contributed to the general discussions.

Conflict of interest   These authors declare no conflict of interest.

Supplementary information   Supporting data are available in the online version of the paper.

Zhe Zheng received his Bachelor degree from Tianjin University in 2014 and is a doctoral candidate at Tianjin University now. His research interest focuses on the separation of semiconducting carbon nanotubes and their applications in field-effect transistors with conjugated polymers.

Huanli Dong received her PhD degree from the Institute of Chemistry, Chinese Academy of Sciences (ICCAS) in 2009. Now she is a professor of the Key Laboratory of Organic Solids, ICCAS. She has received the Outstanding Young Scientist Foundation of NSFC (2012), the Prize for Young Chemists of Chinese Chemical Society (2014) and the National Science Fund for Distinguished Young Scholars (2017). Her research interest focuses on organic polymers and crystals devices, especially optoelectronics.

Jin Zhang received his PhD degree from Lanzhou University in 1997. He has been a professor of Peking University since 2006. He received the National Science Fund for Distinguished Young Scholars (2007), was selected as a Cheung Kong Professor of the Ministry of Education, China (2012), and Ten-Thousand Talents Program Innovation Leaders of the Ministry of Science and Technology (2017). He is mainly engaged in the control synthesis, application and Raman spectroscopy of nano-carbon materials.

Wenping Hu received his PhD from ICCAS in 1999. He is a professor of the School of Science, Tianjin University. And he received the National Science Fund for Distinguished Young Scholars (2007), was selected as a Cheung Kong Professor of the Ministry of Education, China (2014) and Ten-Thousand Talents Program Innovation Leaders of the Ministry of Science and Technology (2016). His research focuses on organic optoelectronics.

碳纳米管辅助共轭聚合物薄膜链间载流子传输以提高迁移率

郑哲[1,2]，倪振杰[2]，张小涛[1]，甄永刚[2]，董焕丽[2*]，张锦[3*]，胡文平[1,2*]

摘要 在过去的几十年中，共轭聚合物因其在光电器件中的广泛应用受到广泛关注．共轭聚合物中的电荷传输过程主要由链内和链间两部分组成，其中链间电荷传输通常低于链内传输，并且可能降低整个电荷运输性质．针对该问题，本文提出了将半导体单壁碳纳米管(s-SWNTs)作为共轭聚合物链间的有效电荷传输通道以改善电荷传输性能的概念．使用典型的共轭聚合物PDPP-TT作为示例，将优化的PDPP-TT/s-SWNTs与纯PDPP-TT薄膜的器件相比，器件性能明显提高，空穴迁移率从2.32增加到12.32 cm^2 V^{-1} s^{-1}，而电子迁移率从2.02增加到5.77 cm^2 V^{-1} s^{-1}．该结果表明在共轭聚合物薄膜中形成连续导电通道的重要性，此概念也可以扩展到其他聚合物器件中，以推进其在大面积、低成本、高性能聚合物电子器件和电路中的应用．